Organic LETTERS

Letter

pubs.acs.org/OrgLett

Synthesis and Properties of Cholesteric Click-Phospholes

Xiaoming He, Jian-Bin Lin, Wang Hay Kan, Simon Trudel, and Thomas Baumgartner*

Department of Chemistry & Centre for Advanced Solar Materials, University of Calgary, 2500 University Drive NW, Calgary, AB T2N 1N4, Canada

Supporting Information

ABSTRACT: Inspired by naturally occurring helical supramolecular architectures, a series of chiral conjugated phospholes with a cholesteryl pendant have been synthesized and characterized. The photophysically and electrochemically active conjugated phosphole species can act as dopants for the formation of chiral liquid crystals. The supramolecular structures were found to be tunable by careful choice of the conjugated headgroup as well as the rigidity of the linker of the new cholesteric phospholes.

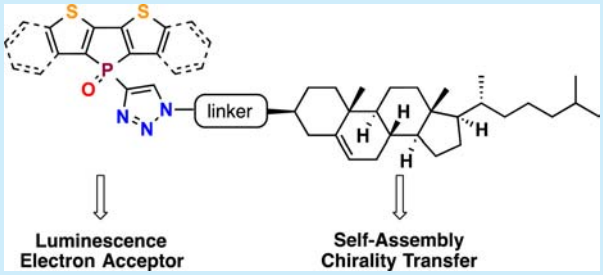

Controlling the architecture of supramolecular assemblies has paramount importance in nature.[1] Biomolecules utilize various weak interactions, such as H-bonding, $\pi-\pi$ interactions, and van der Waals forces, to control supramolecular architectures and to realize vital biological activities. Some typical examples include the double helix of DNA and the bilayer of phospholipids.[1] By mimicking these naturally occurring systems, synthetic chemists have been able to achieve the design of intriguing functional organic materials with relevance to the fields of pharmacy, biochemistry, optical devices, etc.[2] For example, inspired by the natural amphiphilic phospholipids, the groups of Weiss[3] and Kato[4] pioneered the study of the self-assembly of ionic phosphonium compounds (**I**, Figure 1).

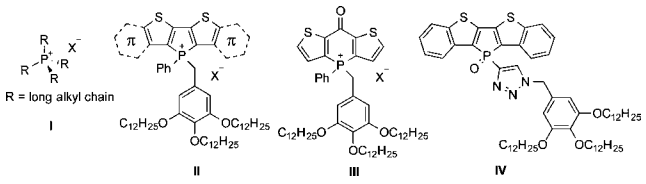

Figure 1. Representative structures of previously reported self-assembled, nonconjugated (**I**) and conjugated (**II**–**IV**) artificial phosphorus-based 'lipids'.

The exploration of conjugated cyclic organophosphorus species is an emerging field of research, because of their promising photophysical and electrochemical properties.[5] Over the past decade, our group's research has been dedicated to the development of novel conjugated organophosphorus species, such as dithieno[3,2-*b*:2′,3′-*d*]phosphole, dithieno[3,2-*c*:2′,3′-*e*]-2,7-diketophosphepin, and dithieno[2,3-*b*;3′,2′-*e*]-4-keto-1,4-dihydrophosphinine.[6−9] We have recently expanded our research by combining the valuable photophysical features of these conjugated organophosphorus systems with the amphiphilic features of lipids to generate self-assembled materials, such as the phosphole- (**II** and **IV**) and phosphinine-lipids (**III**), giving rise to organogels and liquid crystal (LC) mesophases with intriguing photophysical and electrochemical behavior.[8−11a] However, the studies so far have exclusively been focused on achiral self-assembly systems.

Control over the secondary structure and self-assembly of chiral molecules and polymers has been intensively studied over the past few decades.[2,12] One prominent example is the induction of chiral LC phases by doping a small amount of chiral molecules into an achiral nematic liquid crystal.[13] Most chiral organic dopants are based on purely organic materials and chiral molecules with inorganic main group elements (e.g., B, Si, P) remain fairly underexplored to date, mainly because of the synthetic challenges involved. In one of the few examples, Nozaki et al. reported an interesting class of chiral λ^5-phospha[7]helicenes.[14] We thus anticipated that introducing both chirality and self-assembly into conjugated phosphole materials would lead to interesting supramolecular architectures and, moreover, potentially intriguing optoelectronic features.[8−11]

Herein, we now report our initial studies on a series of novel cholesteric conjugated phosphole oxides (Scheme 1). We have selected cholesterol because of its potential for strong hydrophobic interactions and its unique chiral features.[15] Based on the vital role that cholesterol plays for cell membrane function and its interaction with phospholipids, the added optoelectronic properties of the new species may potentially also be utilized as probes for such environments.[16] To the best of our knowledge, this is the first account of conjugated phosphole materials covalently linked to a chiral unit.[17] Furthermore, we demonstrate that these phospholes can act as dopants for the formation of chiral (cholesteric) liquid crystals.

Received: January 14, 2014
Published: February 14, 2014

   dx.doi.org/10.1021/ol500129p | *Org. Lett.* 2014, 16, 1366–1369

Scheme 1. Synthesis of Cholesteric Phosphole Oxides 1a,b and 2a,b

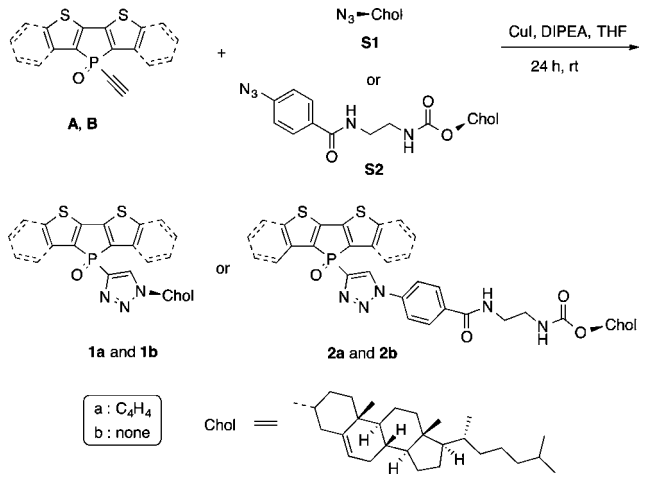

The new compounds were synthesized from the corresponding alkynyl phospholes (**A**, **B**) via a Huisgen "click" protocol (Scheme 1). Compounds **1a,b** and **2a,b** were obtained in moderate yield (45−60%) as yellow (**a** series) and white (**b** series) solids from the corresponding alkynyl phospholes (**A** and **B**) with the corresponding azide (**S1** and **S2**), in adaptation from our previously reported procedure.[11] All new compounds were fully characterized by ^{1}H, ^{13}C, and ^{31}P NMR spectroscopy, as well as mass spectrometry (for details see the Supporting Information (SI)).

Suitable single crystals for X-ray crystallography of **1a** were obtained from slow evaporation of its solution in chloroform and hexane (1:1) at rt. Figure 2 shows its molecular structure and solid-state packing. The crystal data and structure refinement, as well as selected bond lengths and angles, are summarized in Tables S1 and S2 in the SI. Compound **1a** crystallizes in the chiral C_2 space group; the unit cell contains two independent molecules, which differ in the orientation of the phosphole headgroup, arranged in head-to-tail fashion, and the resulting antiparallel pairs are the basis for monolayers in the crystal. The layers stacked on top of each other with a rotation of 90° between them, de facto creating a helical conformation for the stack (4 layers) with a half pitch distance of ca. 26 Å. It is noteworthy that cholesteryl-containing compounds with such an arrangement are very rare in the literature.[18] In the single crystals of **1a**, the phosphorus center adopts a typical pyramidal geometry similar to other phosphole systems.[5−11] The pentacene portion is slightly bent toward the cholesteryl moiety. Our previously reported related achiral heteropentacene dithienophosphole systems revealed some unique O−S interactions and an associated highly ordered edge-to-face arrangement.[6b,11a] However, a similar organization is not observed for **1a**, probably due to the dominating effect of the commonly rigid cholesteryl moiety.[19]

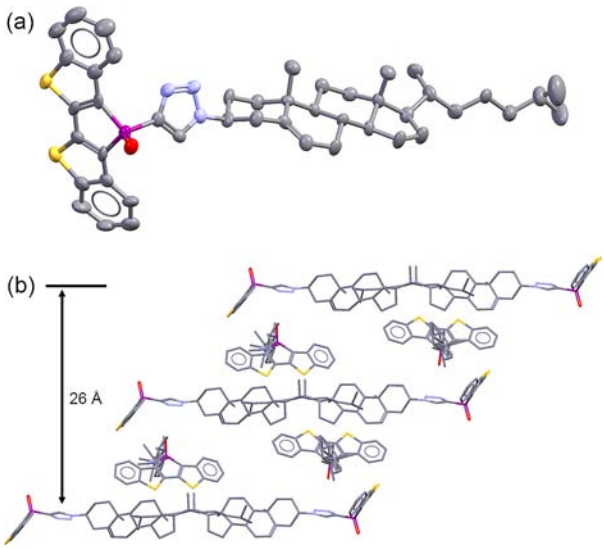

Figure 2. (a) Molecular structure of **1a** (50% probability, H atoms, $CHCl_3$, and second independent molecule omitted for clarity) and (b) 'helical' layer structure of **1a** in the solid state. For crystal data, the bond lengths, and angles, see the SI.

It should be noted in this context that none of the four new compounds show liquid crystalline behavior themselves. Figure S2 shows the scanning electron microscopy (SEM) images of **1a**, **2a**, and **1b**, obtained from their suspensions in CH_2Cl_2/hexanes. Spherical micellar, 2D-crystalline, and 2D-film micromorphologies are observed for **1a**, **2a**, and **1b**, respectively, that are dependent on the π-conjugated headgroups and linkers, highlighting the impact of these two structural elements.

The photophysical and electrochemical data of compounds **1a,b** and **2a,b** are summarized in Table 1, and the spectra are shown in the SI. In line with previously reported relatives,[6,11] the new species are highly fluorescent with quantum yields in the range of ϕ_{PL} = 0.5−0.7 and photophysical properties that are governed by the headgroups. Compounds **1a** (λ_{abs} = 405 nm, λ_{em} = 502 nm) and **2a** (λ_{abs} = 395 nm, λ_{em} = 507 nm) with a larger headgroup exhibit red-shifted photophysics compared to **1b** (λ_{abs} = 365 nm, λ_{em} = 456 nm) and **2b** (λ_{abs} = 370 nm, λ_{em} = 459 nm) with smaller headgroups. Moreover, the two heteropentacene systems **1a** (E_{red} = −1.95 V) and **2a** (E_{red} = −1.90 V) show fully reversible electrochemical reduction behavior (for CVs, see SI) that suggests potential utility for these species as biocompatible, multiresponsive sensory materials.

Table 1. Photophysical and Electrochemical Data for 1a,b and 2a,b

compd	λ_{abs}[a] [nm] (ε [dm^3 mol^{-1} cm^{-1}])	λ_{em} [nm] (ϕ_{PL})[b]	E_{red}[c] [V]
1a	405 (13 750)	502 (0.70)	−1.95
1b	365 (7660)	456 (0.61)	NA
2a	395 (12 920)	507 (0.55)	−1.90
2b	370 (6690)	459 (0.50)	NA

[a]In CH_2Cl_2 solution at 298 K. [b]Fluorescence quantum yield, relative to quinine sulfate (0.1 M H_2SO_4 solution). [c]Half-potentials versus Fc/Fc$^+$, 0.1 M nBu$_4$NPF$_6$ as supporting electrolyte, in CH_2Cl_2. NA: not available.

Doping of nematic LC phases (N) with chiral molecules is known to induce transformation into chiral nematic (or cholesteric; N^*) LC phases through an elasticity approach (Scheme 2). Based on the chiral arrangement of **1a** in the single crystals, we expected the new cholesteric phospholes to be chiral dopants for liquid crystals as well. To verify this, we have selected a commercially available achiral nematic LC, *N*-(4-methoxy-benzilidene)-4-butylaniline (MBBA), shown in Figure 3a, in a proof-of-principle study. The liquid crystal properties of MBBA and the induction of a chiral nematic liquid crystal phase

dx.doi.org/10.1021/ol500129p | Org. Lett. 2014, 16, 1366−1369

Scheme 2. Schematic Pictures Showing (A) the Induction of Chiral Nematic Liquid Crystals and (B) Homeotropic Alignment of Helical Axis to the Substrate

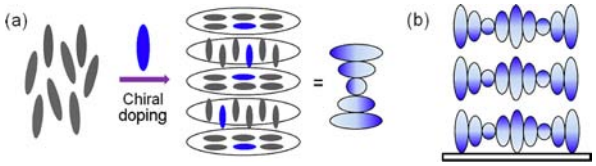

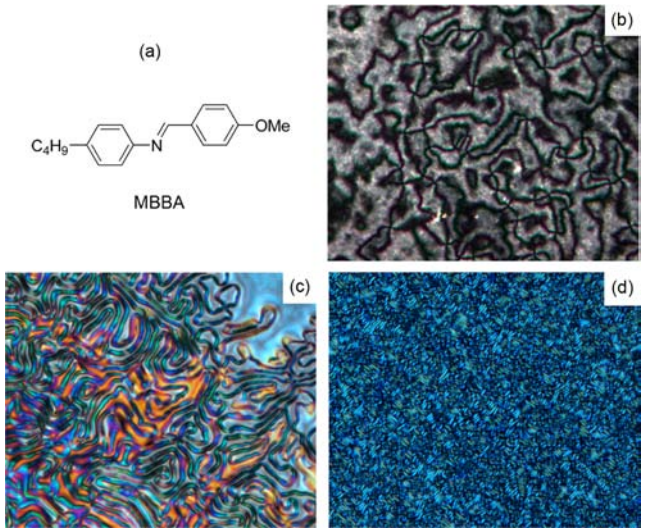

Figure 3. (a) Molecular structure of MBBA, as well as polarized optical micrographs of (b) MBBA, (c) **1a**/MBBA, and (d) **1b**/MBBA. MBBA was doped with 5 wt % of **1a** or **1b**, respectively.

via doping with the new phospholes were investigated. Figure 3 shows the polarized optical microscopy (POM) images of MBBA without and with 5 wt % of **1a** or **1b**. In the absence of the chiral dopants, a typical Schlieren texture is observed for MBBA (Figure 3b). Clear evidence for the formation of a chiral nematic LC phase is provided by the distinct changes in the POM images. A so-called fingerprint texture was observed upon doping MBBA with **1a** and **1b**. The observed fingerprint texture indicates that the helical axis of the chiral nematic phase is parallel to the substrate (Scheme 2b).[20]

In addition, the distances between the striae in the fingerprint texture of **1a**/MBBA (Figure 3c) are much larger than those for **1b**/MBBA (Figure 3d), suggesting the larger helical pitch length for the former.[21] This phenomenon can be attributed to a weaker chiral induction from the hetero-pentacene headgroup in **1a**. Compounds **2a** and **2b** with a flexible linker were also investigated by POM (Figure S6). The texture of **2a**/MBBA is similar to that of **1a**/MBBA; by contrast, no clear fingerprint structures were observed for **2b**/MBBA. All of the above indicates both the headgroups and the linker of this series play a considerable role in the formation of the resulting morphologies. As a control experiment, we also investigated the POM of MBBA doped with cholesterol (Figure S7); a similar fingerprint texture was observed, albeit with very large striae. These results suggest that the presence of the phosphole headgroups strengthens the induction of chirality. Such a unique material-dependent fingerprint texture could be promising for application in security devices, such as ID cards.[22]

The results from the POM were further supported by differential scanning calorimetry (DSC, Figure S8); the analysis of corresponding phase transitions is summarized in Figure 4. As expected, MBBA shows a nematic LC phase between 20 and

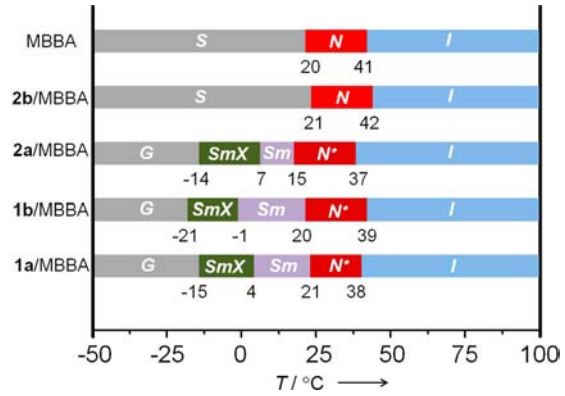

Figure 4. Summary of the LC phase transitions of MBBA with and without doping with 5 wt % **1a,b** and **2a,b**. *S*, solid; *Sm*, smectic; *SmX*, soft crystal; *I*, isotropic; *G*, glassy; *N*, nematic; *N**, chiral nematic.

41 °C. Upon increasing the temperature beyond 41 °C, MBBA transitions into an isotropic liquid, where dark homeotropic areas are observed. By doping MBBA with **1a**, **1b**, and **2a**, respectively, the isotropic temperatures were found to decrease (T_{iso} = 38, 39, and 37 °C for **1a**/MBBA, **1b**/MBBA, and **2a**/MBBA, respectively); the mixture **2b**/MBBA exhibited a slight T_{iso} increase (T_{iso} = 42 °C). The variations can be attributed to different morphologies in each sample. Interestingly, upon heating the samples from −50 to ca. 20 °C, two new phase transitions were observed for MBBA doped with **1a**, **1b**, and **2a**. First, a large exothermic transition is observed at −15 °C (**1a**/MBBA), −21 °C (**1b**/MBBA), and −14 °C (**2a**/MBBA), respectively, which can be ascribed to a glass-to-soft crystal transition in each sample. Continued heating leads to small endothermic peaks at +4, −1, and +7 °C, consistent with a soft-crystal-to-smectic LC phase transition. Subsequently, at higher temperatures (15−21 °C), a smectic-to-cholesteric phase transition is observed, followed by the formation of the isotropic liquid. By heating the sample to the isotropic phase, the optical textures disappear, but can be recovered by cooling the samples down to their cholesteric phases. By contrast, the DSC trace of **2b**/MBBA is similar to that of pure MBBA (Figure S8), suggesting its reduced ability for efficiently inducing chiral liquid crystal morphologies.

To gain further structural information on the LC phases, powder X-ray diffraction (PXRD) studies were carried out (Figure S9). Typically, a sharp, strong peak at low angle ($1° < 2\theta < 4°$) is indicative of smectic phases, while a broad peak at wide angle ($16° < 2\theta < 20°$) appears for nematic, smectic, and cholesteric phases.[23] MBBA itself only shows a broad peak at $2\theta = 20°$; similar spectra are also observed for **1a**/MBBA and **2a**/MBBA. In addition to the broad wide angle, doping with **1b** also gives rise to three new peaks at low angles (2θ = 1.28°, 3.72°, and 7.50°). The appearance of both wide and low angle diffraction is probably due to mixed cholesteric and smectic mesophases, with the former being dominant. This observation supports the proposed LC phase transitions. However, the powder X-ray diffractogram of **2b**/MBBA is likely the simple combination of solid **2b** (Figure S9) and MBBA, indicating the absence of molecular reorganization in the mixture **2b**/MBBA and further supporting the weak ability of **2b** for inducing chirality.

dx.doi.org/10.1021/ol500129p | *Org. Lett.* 2014, 16, 1366−1369

In summary, a series of chiral phospholes appended with a cholesteryl moiety has been designed and synthesized. A helically layered supramolecular organization was confirmed by single-crystal X-ray crystallography. The new compounds have been demonstrated to act as dopants toward chiral liquid crystalline phases, whose supramolecular architecture in the mesophase was determined by the conjugated headgroups and the linkers. This study thus provides a solid foundation for the further study of the self-assembly of chiral phosphole-lipids. Due to the promising photophysical and electrochemical properties of the cholesteric phospholes, we also envision the potential for these materials in optoelectronic applications, such as displays, electrically tunable liquid crystals, and biomolecular sensing probes.

■ ASSOCIATED CONTENT

Supporting Information

Experimental details; ^{1}H, ^{13}C, and ^{31}P NMR spectra of **S2**, **1a**−**1b**, and **2a**−**1b**; X-ray crystal data, structure refinement and selected bonds and angles for **1a**; absorption and emission spectra, cyclic voltammograms, DSC traces, SEM images, and PXRD data. This material is available free of charge via the Internet at http://pubs.acs.org.

■ AUTHOR INFORMATION

Corresponding Author

*E-mail: thomas.baumgartner@ucalgary.ca.

Notes

The authors declare no competing financial interest.

■ ACKNOWLEDGMENTS

Financial support by NSERC of Canada and the Canada Foundation for Innovation (CFI) is gratefully acknowledged.

■ REFERENCES

(1) (a) Whitesides, G. M.; Grzybowski, B. *Science* **2002**, *295*, 2418−2421. (b) Lehn, J. M. *Proc. Natl. Acad. Sci. U.S.A.* **2002**, *99*, 4763−4768. (c) Aizenberg, J.; Fratzl, P. *Adv. Mater.* **2009**, *21*, 387−388. (d) Sanchez, C.; Arribart, H.; Giraud Guille, M. M. *Nat. Mater.* **2005**, *4*, 277−288.

(2) (a) Maeda, K.; Yashima, E. *Top. Curr. Chem.* **2006**, *265*, 47−88. (b) Cornelissen, J. J. L. M.; Rowan, A. E.; Nolte, R. J. M.; Sommerdijk, N. A. J. M. *Chem. Rev.* **2001**, *101*, 4039−4070.

(3) (a) Abdallah, D. J.; Robertson, A.; Hsu, H.-F.; Weiss, R. G. *J. Am. Chem. Soc.* **2000**, *122*, 3053−3062. (b) Chen, H.; Kwait, D. C.; Gönen, Z. S.; Weslowski, B. T.; Abdallah, D. J.; Weiss, R. G. *Chem. Mater.* **2002**, *14*, 4063−4072. (c) Ma, K.; Shahkhatuni, A. A.; Somashekhar, B. S.; Gowda, G. A. N.; Tong, Y.; Khetrapal, C. L.; Weiss, R. G. *Langmuir* **2008**, *24*, 9843−9854.

(4) Ichikawa, T.; Yoshio, M.; Hamasaki, A.; Taguchi, S.; Liu, F.; Zeng, X.-b.; Ungar, G.; Ohno, H.; Kato, T. *J. Am. Chem. Soc.* **2012**, *134*, 2634−2643.

(5) (a) Baumgartner, T.; Réau, R. *Chem. Rev.* **2006**, *106*, 4681−4727. (b) Crassous, J.; Réau, R. *Dalton Trans.* **2008**, 6865−6876. (c) Matano, Y.; Imahori, H. *Org. Biomol. Chem.* **2009**, *7*, 1258−1271. (d) Ren, Y.; Baumgartner, T. *Dalton Trans.* **2012**, *41*, 7792−7800.

(6) (a) Baumgartner, T.; Neumann, T.; Wirges, B. *Angew. Chem., Int. Ed.* **2004**, *43*, 6197−6201. (b) Dienes, Y.; Eggenstein, M.; Kárpáti, T.; Sutherland, T. C.; Nyulászi, L.; Baumgartner, T. *Chem.—Eur. J.* **2008**, *14*, 9878−9889.

(7) He, X. M.; Woo, A. Y. Y.; Borau-Garcia, J.; Baumgartner, T. *Chem.—Eur. J.* **2013**, *19*, 7620−7630.

(8) He, X. M.; Lin, J.-B.; Kan, W. H.; Baumgartner, T. *Angew. Chem., Int. Ed.* **2013**, *52*, 8990−8994.

(9) He, X. M.; Borau-Garcia, J.; Woo, A. Y. Y.; Trudel, S.; Baumgartner, T. *J. Am. Chem. Soc.* **2013**, *135*, 1137−1147.

(10) (a) Ren, Y.; Kan, W. H.; Henderson, M. A.; Bomben, P. G.; Berlinguette, C. P.; Thangadurai, V.; Baumgartner, T. *J. Am. Chem. Soc.* **2011**, *133*, 17014−17026. (b) Ren, Y.; Kan, W. H.; Thangadurai, V.; Baumgartner, T. *Angew. Chem., Int. Ed.* **2012**, *51*, 3964−3968.

(11) (a) He, X. M.; Lin, J.-B.; Kan, W. H.; Dong, P.; Trudel, S.; Baumgartner, T. *Adv. Funct. Mater.* **2014**, *24*, 897−906. (b) He, X. M.; Zhang, P.; Lin, J.-B.; Huynh, H. V.; Navarro Muñoz, S. E.; Ling, C.-C.; Baumgartner, T. *Org. Lett.* **2013**, *15*, 5322−5235.

(12) (a) Engelkamp, H.; Middelbeek, S.; Nolte, R. J. M. *Science* **1999**, *284*, 785−788. (b) Jin, W.; Fukushima, T.; Niki, M.; Kosaka, A.; Ishii, N.; Aida, T. *Proc. Natl. Acad. Sci. U.S.A.* **2005**, *102*, 10801−10806. (c) Miyagawa, T.; Furuko, A.; Maeda, K.; Katagiri, H.; Furusho, Y.; Yashima, E. *J. Am. Chem. Soc.* **2005**, *127*, 5018−5019.

(13) (a) Pieraccini, S.; Masiero, S.; Ferrarini, A.; Spada, G. P. *Chem. Soc. Rev.* **2011**, *40*, 258−271. (b) Su, X.; Voskian, S.; Hughes, R. P.; Aprahamian, I. *Angew. Chem., Int. Ed.* **2013**, *52*, 10734−10739. (c) Yoshida, J.; Watanbe, G.; Kakizawa, K.; Kawabata, Y.; Yuge, H. *Inorg. Chem.* **2013**, *52*, 11042−11050. (d) Rosini, C.; Spada, G. P.; Proni, G.; Masiero, S.; Scamuzzi, S. *J. Am. Chem. Soc.* **1997**, *119*, 506−512. (e) Seed, A. J.; Walsh, M. E.; Doane, J. W.; Khan, A. *Mol. Cryst. Liq. Cryst.* **2004**, *410*, 201−208. (f) Frank, B. B.; Camafort Blanco, B.; Jakob, S.; Ferroni, F.; Pieraccini, S.; Ferrarini, A.; Boudon, C.; Gisselbrecht, J.-P.; Seiler, P.; Spada, G. P.; Diederich, F. *Chem.—Eur. J.* **2009**, *15*, 9005−9016. (g) Goh, M.; Park, J.; Han, Y.; Ahn, S.; Akagi, K. *J. Mater. Chem.* **2012**, *22*, 25011−25018.

(14) Nakano, K.; Oyama, H.; Nishimura, Y.; Nakasako, S.; Nozaki, K. *Angew. Chem., Int. Ed.* **2012**, *51*, 695−699.

(15) (a) Ajayaghosh, A.; Praveen, V. K.; Vijayakumar, C. *Chem. Soc. Rev.* **2008**, *37*, 109−122. (b) Yang, X.; Zhang, G.; Zhang, D. *J. Mater. Chem.* **2012**, *22*, 38−50. (c) George, M.; Weiss, R. G. *Acc. Chem. Res.* **2006**, *39*, 489−497. (d) Li, Y.; Lam, E. S. H.; Tam, A. Y. Y.; Wong, K. M. C.; Lam, W. H.; Wu, L.; Yam, V. W. W. *Chem.—Eur. J.* **2013**, *19*, 9987−9994.

(16) Robalo, J. R.; Ramalho, J. P. P.; Loura, L. M. S. *J. Phys. Chem. B* **2013**, *117*, 13731−13742.

(17) Chiral phosphole ligands have been reported before; see for example: Ogasawara, M.; Yoshida, K.; Hayashi, T. *Organometallics* **2001**, *20*, 1014−1019.

(18) (a) Ostuni, E.; Kamaras, P.; Weiss, R. G. *Angew. Chem., Int. Ed.* **1996**, *35*, 1324−1326. (b) Soulivong, D.; Matt, D.; Ziessel, R. *Chem. Commun.* **1999**, 393−394.

(19) (a) Pucci, D.; Aiello, I.; Bellusci, A.; Crispini, A.; De Franco, I.; Ghedini, M.; La Deda, M. *Chem. Commun.* **2008**, 2254−2256. (b) Ohta, H.; Fujihara, T.; Tsuji, Y. *Dalton Trans.* **2008**, 379−385. (c) Kohmoto, S.; Okuyama, S.; Nakai, T.; Takahashi, M.; Kishikawa, K.; Masu, H.; Azumaya, I. *J. Mol. Struct.* **2011**, *998*, 192−197.

(20) Despite the observed chirality in the LC phase, the species did not show any Circular Dichroism (CD).

(21) Piao, G.; Akagi, K.; Shirakawa, H.; Kyotani, M. *Curr. Appl. Phys.* **2001**, *1*, 121−123.

(22) Nakayama, K.; Ohtsubo, J. *Mol. Cryst. Liq. Cryst.* **2010**, *516*, 253−259.

(23) Zhang, B. Y.; Hu, J. S.; Jia, Y. G.; Du, B. G. *Macromol. Chem. Phys.* **2003**, *204*, 2123−2129.